doi:10.1038/nature24273

Supplementary Methods

1. Modeling coevolution in mutualistic networks

1.1. Model description

Recently, a set of studies has started to explore evolutionary dynamics in mutualistic networks, which are major components of all biologically diverse ecosystems. These studies are rooted in distinct modeling approaches, including models based on assembly rules[15], adaptive dynamics models[31,32], genetic population models[14], individual-based models[14], and stochastic[16] and deterministic[33] network models that describe traits as quantitative node states. These studies have allowed us to begin to understand how coevolution shapes and is shaped by network patterns, revealing the link between evolutionary dynamics and ecological dynamics[31,32], the role of linkage rules and trait evolution in shaping network patterns[14,15], the effects of specific lifestyles on evolutionary change[16], and the feedback between network structure and trait evolution[33]. In this paper, we move toward a new modeling approach by analyzing how natural selection acts both directly and indirectly within assemblages of species. Our new modeling approach has two main elements: a coevolutionary model for networks based on selection gradients and the analytical derivation of the coevolutionary matrix. As previous coevolutionary networks models[14,16,33], our model is a time-discrete model that describes trait evolution in the context of selection imposed by environment and species interactions[14,33]. However, by using selection gradients in coevolutionary network models, our model allows an explicit connection between trait evolution and changes in the adaptive landscape. The description of coevolution as the reorganization of adaptive landscapes due to species interactions[34] leads to the second component of our modeling approach, the analytical derivation of the coevolutionary matrix (**T** matrix). The coevolutionary matrix is a matrix that integrates trait evolution, species interactions, reciprocal direct and indirect evolutionary effects, and the reorganization of the adaptive peaks. This new approach allows an assessment, for the first time, of how indirect interactions reshape adaptive landscapes in mutualistic networks and, in doing so, (1) contribute to the relentless evolution of interactions, (2) alter the process of reciprocal change differently in intimate interactions and multiple-partner interactions, (3) change the pace of directional evolutionary change, and (4) affect the reorganization of mutualisms over time.

In our model, a local network was formed by N species, each of which was represented by a single population. As a first approximation, we assumed short time scales, and we studied the coevolutionary dynamics of local assemblages of interacting species. Recent studies show that rapid evolution can occur in species-rich mutualisms (e.g., Ref. 3), and this assumption allowed us to focus on trait evolution while ignoring other aspects of the evolutionary dynamics, such as speciation. Thus, we assumed that species richness, N, was fixed and that the population of species i was formed by n_i individuals. Each individual h of species i was characterized by a single trait value, Z_{ih}. In nature, Z_{ih} may refer to a quantitative trait that mediates the interaction between individuals of different species, such as the length of a hummingbird's bill or a flower's corolla. Alternatively, Z_{ih} can be viewed as set of traits evolving together because of strong genetic integration[35], such as multiple traits in fruits that are also functionally associated with each other[36]. We assumed that Z_{ih} affects the fitness benefits derived from the mutualistic interactions with individuals of interacting species. In addition to mutualism, we also assumed that Z_{ih} affects other aspects of fitness of the individuals in the environment. Thus, we assumed that Z_{ih} was under selection by distinct environmental and mutualism selective pressures because the traits involved in interactions are always under distinct selective pressures[2,37].

We then defined $Z_i^{(t)}$ as the mean value of a single quantitative trait in a given species i at time t, $Z_i^{(t)} = \sum_{h=1}^{n_i} Z_{ih}/n_i$. In our simulations, we adopted a mean-field approach to describe trait values and directly modeled the evolutionary dynamics of $Z_i^{(t)}$ in a manner similar to classical studies of directional selection[38]. This assumption allowed us to derive a coevolutionary matrix connecting mean species traits to the phenotypes favored by environmental selection (see 1.2 Coevolutionary matrix). We assumed that the phenotypic variance of $Z_i^{(t)}$, $\sigma_{Z_i}^2$, is fixed, which is a useful approximation for large population sizes. We assumed that $Z_i^{(t)}$ shaped the patterns of interaction of species i with other species in the network, thus allowing evolutionary feedback between traits and patterns of interaction. Evolutionary change in a given time step of $Z_i^{(t)}$ was derived using the classical equation for phenotypic evolution[38]:

$$\Delta Z_i^{(t)} = h_{Z_i}^2 \sigma_{Z_i}^2 \frac{\partial \ln \bar{W}_i}{\partial Z_i} \quad \text{(S1)}$$

where $h^2_{Z_i}$ is the heritability of trait $Z_i^{(t)}$, which was assumed to be constant over time, $\sigma^2_{Z_i}$ is the phenotypic variance of $Z_i^{(t)}$, which was also assumed to be constant through time, and $\frac{\partial \ln \bar{W}_i}{\partial Z_i}$ is the selection gradient. The selection imposed by the mutualisms and environment effects may lead to very complex adaptive landscapes in which the adaptive peaks vary across time[34]. We assumed that the adaptive landscape at a given time step t is formed by a single adaptive peak, but we incorporated the temporal variation in the adaptive peaks, which were continually reshaped by the trait evolution of the other species in the network. To do this, we assumed a linear selection gradient defined as:

$$\frac{\partial \ln W_i}{\partial Z_i} = \varrho_i \left(Z_{i,p}^{(t)} - Z_i^{(t)} \right) \quad \text{(S2)}$$

where ϱ_i is a scaling constant affecting the sensitivity of $\bar{W}_i$ to changes in $Z_i^{(t)}$, and $Z_{i,p}^{(t)}$ is the mean trait value defining the adaptive peak of the population of species i at time step t. We decomposed $Z_{i,p}^{(t)}$ into the trait values favored by environmental and mutualistic selection:

$$Z_{i,p}^{(t)} = \sum_{j,j\neq i}^{N} q_{ij}^{(t)} X_{ij}^{(t)} + \left(1 - \sum_{j,j\neq i}^{N} q_{ij}^{(t)}\right) \theta_i^{(t)} \quad \text{(S3)}$$

The coefficient $q_{ij}^{(t)}$ is the evolutionary effect of a mutualistic interaction, weighting the relative importance of the selection imposed by species j to the selection gradient compared with all of other potential selective pressures, $0 \leq q_{ij}^{(t)} \leq 1$. $X_{ij}^{(t)}$is the mean trait value of species i favored by the selection imposed by individuals of species j. The term $1 - \sum_{j,j\neq i}^{N} q_{ij}^{(t)}$ weights the relative importance of environmental selection to the selection gradient. Environmental selection is the sum of the effects of all selective pressures that are not related to mutualisms. Finally, $\theta_i^{(t)}$ is the mean trait value for species i that is favored by environmental selection. By combining equations S1, S2, and S3 and considering that $h^2_{Z_i} = \sigma^2_{G_{Z_i}} / \sigma^2_{Z_i}$, in which $\sigma^2_{G_{Z_i}}$ is the additive genetic variance of trait $Z_i^{(t)}$, the temporal dynamics of the traits could be described as follows:

$$Z_i^{(t+1)} = Z_i^{(t)} + \varphi_i \left[\sum_{j,j\neq i}^{N} q_{ij}^{(t)} \left(X_{ij}^{(t)} - Z_i^{(t)} \right) + \left(1 - \sum_{j,j\neq i}^{N} q_{ij}^{(t)}\right) \left(\theta_i^{(t)} - Z_i^{(t)} \right) \right] \quad \text{(S4)}$$

in which φ_i is a compound parameter $\varphi_i = \sigma^2_{G_{Z_i}} \varrho_i$. We assumed that the trait value

favored by environmental selection is fixed over time, $\theta_i^t = \theta_i$. We later explored the effects of environmental fluctuations on trait evolution (Fig. 4, main text). We also assumed that selection imposed by mutualistic partners favors complementarity among interacting partners, as in previous coevolutionary models for mutualistic networks[14,16]. Maximal complementarity would occur under extreme phenotypic matching between interacting partners. For simplicity, we defined maximal phenotypic matching as $Z_j^{(t)} = Z_i^{(t)}$; therefore, $X_{ij}^{(t)} = Z_j^{(t)}$, which leads to equation (1) of the main text:

$$Z_i^{(t+1)} = Z_i^{(t)} + \varphi_i \left[\sum_{j,j\neq i}^{N} q_{ij}^{(t)} \left(Z_j^{(t)} - Z_i^{(t)}\right) + \left(1 - \sum_{j,j\neq i}^{N} q_{ij}^{(t)}\right)\left(\theta_i - Z_i^{(t)}\right)\right] \quad (1)$$

Using this expression, we can explore how evolutionary effects $q_{ij}^{(t)}$ vary over time. Species interactions are often affected by multiple traits of interacting individuals of different species. As a result, the evolution of any trait is affected by the evolution of other traits that evolve at different rates. We incorporated the consequences of other traits in our model by decomposing the relative importance of selection imposed by a potential partner *j* into two components: (i) $e^{-\alpha\left(Z_j^{(t)} - Z_i^{(t)}\right)^2}$, which is the component of the selection imposed by species *j* mediated by trait $Z_i^{(t)}$, where α describes the sensitivity of the evolutionary effect of the interaction to trait matching, and (ii) $a_{ij}^{(t)}$, which is the component of selection associated with all other traits of *i* that affect the interaction between *i* and *j*, $0 \leq a_{ij}^{(t)} \leq 1$. The combination of these two components leads to:

$$q_{ij}^t = m_i a_{ij}^{(t)} \frac{e^{-\alpha\left(Z_j^{(t)} - Z_i^{(t)}\right)^2}}{\sum_{k,i\neq k}^{N} a_{ik}^{(t)} e^{-\alpha\left(Z_k^{(t)} - Z_i^{(t)}\right)^2}} \quad (S5)$$

where m_i is the level of mutualistic selection and measures the relative importance of all mutualistic interactions as selective pressures on $Z_i^{(t)}$; $0 \leq m_i = \sum_{j,j\neq i}^{N} q_{ij}^t \leq 1$. As a first approximation, we assumed that m_i is constant, but our sensitivity analysis showed that violating this assumption did not qualitatively affect our main results (see section 1.3). We made the simplifying assumption that the genetic covariance between $Z_i^{(t)}$ and the other traits affecting the interaction is negligible, which allowed us to consider $a_{ij}^{(t)}$ and $e^{-\alpha\left(Z_j^{(t)} - Z_i^{(t)}\right)^2}$ as independent components. We also assumed that $Z_i^{(t)}$ evolves at a faster

rate than all of the other traits affecting the mutualism, which allowed the simplification $a_{ij}^{(t)} = a_{ij}$. We later explored this assumption and its potential consequences (see section 1.3). Finally, we assumed that traits affecting a_{ij} exert a barrier effect on the interaction[15], i.e., allowing interactions to occur ($a_{ij} = 1$) or not occur ($a_{ij} = 0$). This assumption did not affect the main conclusions of this study; see *barrier effects* in section 1.3. Thus, our model incorporates the mechanisms of trait matching, $e^{-\alpha\left(z_j^{(t)} - z_i^{(t)}\right)^2}$ and trait barriers (the traits summarized in a_{ij}) that are likely to govern the ecology and evolution of mutualisms[15]. Combining equations S5 and 1 yields the following equation:

$$Z_i^{(t+1)} = Z_i^{(t)} + \varphi_i \left[m_i \sum_{j,j\neq i}^{N} a_{ij} \frac{e^{-\alpha\left(z_j^{(t)} - z_i^{(t)}\right)^2}}{\sum_{k,i\neq k}^{N} a_{ik} e^{-\alpha\left(z_k^{(t)} - z_i^{(t)}\right)^2}} \left(Z_j^{(t)} - Z_i^{(t)}\right) + (1 - m_i)\left(\theta_i - Z_i^{(t)}\right) \right] \quad \text{(S6)}$$

Thus, a_{ij} and $e^{-\alpha\left(z_j^{(t)} - z_i^{(t)}\right)^2}$ represent the fixed and dynamical components of the structure of mutualistic networks, which limit and shape how evolution and coevolution can occur in these networks. In equation S6, $a_{ij} = 0$ represents a forbidden link, which is an interaction that cannot occur[39] and is stable over evolutionary timescales. This potential interaction is a forbidden link because other traits prevent the interaction from occurring regardless of how strong the trait matching is between species $Z_j^{(t)}$ and $Z_i^{(t)}$. Alternatively, a potential interaction may have negligible evolutionary effects even if other traits allowed the interaction to occur ($a_{ij} = 1$). For example, a strong mismatch between $Z_j^{(t)}$ and $Z_i^{(t)}$relative to the matching between i and its other partners would result in $\frac{e^{-\alpha\left(z_j^{(t)} - z_i^{(t)}\right)^2}}{\sum_{k,i\neq k}^{N} a_{ik} e^{-\alpha\left(z_k^{(t)} - z_i^{(t)}\right)^2}} \to 0, q_{ij}^{(t)} \to 0$. In this latter case, the evolutionary effect of the mutualistic interaction between i and j is functionally negligible.

In all of the subsequent analyses, we assumed $0 < \varphi_i < 1$ and $0 < m_i < 1$ for any species i. Using equation 1 of the main text as a starting point, we performed numerical simulations to study the evolutionary dynamics of the model. The evolutionary dynamics converged to equilibrium (Extended Data Fig. 1), regardless the properties of the network used to parameterize the model. Then, we characterized the phenotype of species i at the equilibrium.

We used the simplifying assumption that $q_{ij}^{(t)}$ was fixed, leading to $q_{ij}^{(t)} = q_{ij}$. Under this approximation, the equilibrium is described as:

$$Z_i^* = \sum_j^N q_{ij} Z_j^* + \left(1 - \sum_j^N q_{ij}\right)\theta_i \quad \text{(S7)}$$

For a set of N species, equation S7 can be rewritten in matrix form as follows:

$$\mathbf{Z}^* = \mathbf{Q}\mathbf{Z}^* + \mathbf{\Psi\Theta} = (\mathbf{I} - \mathbf{Q})^{-1}\mathbf{\Psi\Theta} \quad \text{(S8)}$$

where $\mathbf{Z}^*$ is an $Nx1$ vector describing the trait values of each species at the equilibrium, $\mathbf{Q}$ is an NxN matrix in which species are depicted in both rows and columns and nonzero elements represent the direct evolutionary effects of the interacting species in the columns on the mean phenotypes of the species in the rows, $\mathbf{\Psi}$ is an NxN diagonal matrix in which $\psi_{ii} = 1 - m_i$ for any species i, $\mathbf{\Theta} = \{\theta_i; \theta_j;\ \theta_k;\ \ldots; \theta_N\}$ is an $Nx1$ vector describing the trait values favored by environmental selection, and $\mathbf{I}$ is the NxN identity matrix. We investigated the local stability of the model. Equation 1 can be rewritten in matrix form as follows:

$$\mathbf{Z}^{(t+1)} = \left(\mathbf{I} - \mathbf{\Phi} + \mathbf{\Phi}\mathbf{Q}^{(t)}\right)\mathbf{Z}^{(t)} + \mathbf{\Phi\Psi\Theta} \quad \text{(S9)}$$

where $\mathbf{\Phi}$ is an NxN diagonal matrix in which the diagonal elements represent the compound parameter φ_i for each species i, which measures how rapidly a population evolves due to the slope of the selection gradient and the additive genetic variance. We assumed that at time step $t = \tau$, the system is at equilibrium; thus, $\mathbf{Z}^{(\tau)} = \mathbf{Z}^*$ and $\mathbf{Q}^{(t)} \cong \mathbf{Q}$. We performed small perturbations of the trait values of all species, as depicted in the $Nx1$ vector $\mathbf{E} = \{\varepsilon_i; \varepsilon_j;\ \varepsilon_k;\ \ldots; \varepsilon_N\}$. The local stability of the system was governed by:

$$\mathbf{\Delta Z} = (\mathbf{I} - \mathbf{\Phi} + \mathbf{\Phi Q})\mathbf{E} \quad \text{(S10)}$$

The matrix $\mathbf{I} - \mathbf{\Phi} + \mathbf{\Phi Q}$ has N eigenvalues, and these eigenvalues control the stability of the model. The model is stable if all eigenvalues have absolute values less than one. If $0 < \varphi_i < 1$ and $0 < m_i < 1$ for any species i, then the absolute values of all eigenvalues of the matrix $\mathbf{I} - \mathbf{\Phi} + \mathbf{\Phi Q}$ are less than one. As a consequence, the perturbation diminishes, and the equilibrium is stable.

Next, we determined whether the analytical approximation of the model converges to equation S8. Using the simplifying assumption $\mathbf{Q}^{(t)} = \mathbf{Q}$:

$$\mathbf{Z^{(1)}} = (\mathbf{I} - \mathbf{\Phi} + \mathbf{\Phi Q})\mathbf{Z^{(0)}} + \mathbf{\Phi\Psi\Theta} \quad \text{(S11)}$$

$$\mathbf{Z^{(2)}} = (\mathbf{I} - \mathbf{\Phi} + \mathbf{\Phi Q})\mathbf{Z^{(1)}} + \mathbf{\Phi\Psi\Theta} \quad \text{(S12)}$$

$$\mathbf{Z^{(2)}} = (\mathbf{I} - \mathbf{\Phi} + \mathbf{\Phi Q})^{\mathbf{2}}\mathbf{Z^{(0)}} + (\mathbf{I} - \mathbf{\Phi} + \mathbf{\Phi Q})\mathbf{\Phi\Psi\Theta} + \mathbf{\Phi\Psi\Theta} \quad \text{(S13)}$$

For time step τ,

$$\mathbf{Z^{(\tau)}} = (\mathbf{I} - \mathbf{\Phi} + \mathbf{\Phi Q})^{\boldsymbol{\tau}}\mathbf{Z^{(0)}} + \sum_{t=0}^{\tau-1}(\mathbf{I} - \mathbf{\Phi} + \mathbf{\Phi Q})^{\boldsymbol{t}}\mathbf{\Phi\Psi\Theta} \quad \text{(S14)}$$

If the traits of all species are under environmental selection ($m_i < 1$ for any species i), the leading eigenvalue of $(\mathbf{I} - \mathbf{\Phi} + \mathbf{\Phi Q})$ is $0 < \lambda_1 < 1$, implying that ${\lambda_1}^{\boldsymbol{t}} \longrightarrow 0$ for large t, resulting in:

$$(\mathbf{I} - \mathbf{\Phi} + \mathbf{\Phi Q})^{\boldsymbol{\tau}}\mathbf{Z^{(0)}} \to \mathbf{0} \quad \text{(S15)}$$

$$\sum_{t=0}^{\tau-1}(\mathbf{I} - \mathbf{\Phi} + \mathbf{\Phi Q})^{\boldsymbol{t}}\mathbf{\Phi\Psi\Theta} \to (\mathbf{I} - \mathbf{I} + \mathbf{\Phi} - \mathbf{\Phi Q})^{-\mathbf{1}}\mathbf{\Phi\Psi\Theta} \quad \text{(S16)}$$

where $\mathbf{0}$ is a null vector, and $(\mathbf{I} - \mathbf{I} + \mathbf{\Phi} - \mathbf{\Phi Q})^{-\mathbf{1}}$ is the asymptotic sum of all matrices. Substituting S16 and S15 in S14 gives the following:

$$\mathbf{Z^{(\tau)}} = (\mathbf{I} - \mathbf{I} + \mathbf{\Phi} - \mathbf{\Phi Q})^{-\mathbf{1}}\mathbf{\Phi\Psi\Theta} \quad \text{(S17a)}$$

$$\mathbf{Z^{(\tau)}} = (\mathbf{I} - \mathbf{Q})^{-\mathbf{1}}\mathbf{\Psi\Theta} \quad \text{(S17b)}$$

Thus, the analytical approximation assuming fixed evolutionary effects of the model converged to the fixed point predicted in equation S8. We tested whether the analytical predictions held for our numerical simulations in which the evolutionary effects are not fixed but vary over time until reaching equilibrium (n = 10^2 simulations per parameterization using each of the 75 empirical networks; $\langle\varphi\rangle = 0.2 \pm 0.01$, $\langle\theta\rangle = 10$, and $\langle m\rangle = 0.7 \pm 0.01$). We calculated the mean absolute difference between $\mathbf{Z}^*$ and $\mathbf{Z}^E$, where $\mathbf{Z}^*$ is the vector with asymptotic trait values obtained in the numerical simulations, and $\mathbf{Z}^E$ is the vector with trait values based on the analytical prediction, $\mathbf{Z}^E = (\mathbf{I} - \mathbf{Q}^*)^{-\mathbf{1}}\mathbf{\Psi\Theta}$, where $\mathbf{Q}^*$ is the matrix of direct evolutionary effects at the equilibrium and was obtained at the end of the simulations. The simulations corroborated the performance of the analytical approximation: the mean absolute difference between the asymptotic trait value of a given species in the numerical simulation ($\mathbf{Z}^*$) and the trait value predicted by equation S10 ($\mathbf{Z}^E$) was negligible (mean±SD = $6.75\times10^{-4} \pm 5.18\times10^{-4}$, n = *100* simulations for each of the 75 networks).

1.2. Coevolutionary matrix

We used our coevolutionary model to explore how indirect effects affect the coevolutionary dynamics. We defined indirect effects as the contributions of non-interacting species to trait evolution. A non-interacting species is a species that does not directly interact with the focal species. We used our analytical result (equation S8) to explore the contribution of indirect effects to trait evolution. We analyzed the coevolutionary matrix $\mathbf{T} = (\mathbf{I} - \mathbf{Q})^{-1}\mathbf{\Psi}$, which describes how mutualistic interactions reshape the mean phenotypes of each species in the network by creating links between the trait values favored by environmental selection on multiple species (equation S8).

We explored (1) how mutualisms reshape the trait distributions of interacting species and (2) how, in mutualistic networks, the reshaping of trait distributions is associated with indirect effects. We used the three scenarios reported in Fig. 1 (main text) to illustrate these results. In the first scenario (Fig. 1A), the four species did not interact, $m_1 = m_2 = m_3 = m_4 = 0$, therefore:

$$\mathbf{\Psi} = \{1; 1; 1; 1\} \quad \text{(S18a)}$$

$$\mathbf{Z}^* = \{\theta_1; \theta_2;\ \theta_3; \theta_4\} \quad \text{(S18b)}$$

$$\mathbf{T} = \mathbf{I} \quad \text{(S18c)}$$

Equation S18c implies that there was no effect of co-occurring species on the trait values of any given species. In the scenario in which there were two sets of isolated pairwise interactions, there was the potential for effects of interacting species, but no indirect effects, on trait evolution (Fig. 1B). At equilibrium, the fixed trait values for the species were as follows:

$$Z_1^* = q_{12}^* Z_2^* + (1 - q_{12}^*)\theta_1 \quad \text{(S19a)}$$

$$Z_2^* = q_{21}^* Z_1^* + (1 - q_{21}^*)\theta_2 \quad \text{(S19b)}$$

$$Z_3^* = q_{34}^* Z_4^* + (1 - q_{34}^*)\theta_3 \quad \text{(S19c)}$$

$$Z_4^* = q_{43}^* Z_3^* + (1 - q_{43}^*)\theta_4 \quad \text{(S19d)}$$

S19 produced the following:

$$Z_1^* = \frac{q_{12}^*(1-q_{21}^*)\theta_2+(1-q_{12}^*)\theta_1}{1-q_{12}^*q_{21}^*} \quad \text{(S20a)}$$

$$Z_2^* = \frac{q_{21}^*(1-q_{12}^*)\theta_1+(1-q_{21}^*)\theta_2}{1-q_{21}^*q_{12}^*} \quad \text{(S20b)}$$

$$Z_3^* = \frac{q_{34}^*(1-q_{43}^*)\theta_4+(1-q_{34}^*)\theta_3}{1-q_{34}^*q_{43}^*} \quad \text{(S20c)}$$

$$Z_4^* = \frac{q_{43}^*(1-q_{34}^*)\theta_3+(1-q_{43}^*)\theta_4}{1-q_{43}^*q_{34}^*} \quad \text{(S20d)}$$

and:

$$\mathbf{T} = \begin{bmatrix} \frac{1-q_{12}^*}{1-q_{12}^*q_{21}^*} & \frac{q_{12}^*(1-q_{21}^*)}{1-q_{12}^*q_{21}^*} & 0 & 0 \\ \frac{q_{21}^*(1-q_{12}^*)}{1-q_{12}^*q_{21}^*} & \frac{1-q_{21}^*}{1-q_{12}^*q_{21}^*} & 0 & 0 \\ 0 & 0 & \frac{1-q_{34}^*}{1-q_{34}^*q_{43}^*} & \frac{q_{34}^*(1-q_{43}^*)}{1-q_{34}^*q_{43}^*} \\ 0 & 0 & \frac{q_{43}^*(1-q_{34}^*)}{1-q_{34}^*q_{43}^*} & \frac{1-q_{43}^*}{1-q_{34}^*q_{43}^*} \end{bmatrix} \quad \text{(S21)}$$

Therefore, the equilibrium trait values balanced the trait values favored by environmental selection and the reciprocity of the coevolutionary process, $q_{ij}q_{ji}$. However, because the network is formed by two isolated sets of pairwise interactions, there was no indirect effect. We then focused on the coevolution in linear networks (also called path graphs, Fig. 1C) to explore how indirect effects affected trait evolution in species in one of the simplest types of network. At equilibrium, the trait values were defined as:

$$Z_1^* = q_{12}^*Z_2^* + (1-m_1)\theta_1 \quad \text{(S22a)}$$

$$Z_2^* = q_{21}^*Z_1^* + q_{23}^*Z_3^* + (1-m_2)\theta_2 \quad \text{(S22b)}$$

$$Z_3^* = q_{32}^*Z_2^* + q_{34}^*Z_4^* + (1-m_3)\theta_3 \quad \text{(S22c)}$$

$$Z_4^* = q_{43}^*Z_3^* + (1-m_4)\theta_4 \quad \text{(S22d)}$$

We defined the coevolutionary effect as the reciprocity of evolutionary effects:

$$r_{ij} = q_{ij}^*q_{ji}^* \quad \text{(S23)}$$

Using this definition and defining $b = \frac{1}{1-r_{12}-r_{23}-r_{34}+r_{12}r_{34}}$, the matrix $\mathbf{T}$ for the linear, four-species network was as follows:

$$\mathbf{T} = \begin{bmatrix} b(1-m_1)(1-r_{23}-r_{34}) & b(1-m_2)q_{12}^*(1-r_{34}) & b(1-m_3)q_{12}^*q_{23}^* & b(1-m_4)q_{12}^*q_{23}^*q_{34}^* \\ b(1-m_1)q_{21}^*(1-r_{34}) & b(1-m_2)(1-r_{34}) & b(1-m_3)q_{23}^* & b(1-m_4)q_{23}^*q_{34}^* \\ b(1-m_1)q_{21}^*q_{32}^* & b(1-m_2)q_{32}^* & b(1-m_3)(1-r_{12}) & b(1-m_4)q_{34}^*(1-r_{12}) \\ b(1-m_1)q_{21}^*q_{32}^*q_{43}^* & b(1-m_2)q_{32}^*q_{43}^* & b(1-m_3)q_{43}^*(1-r_{12}) & b(1-m_4)(1-r_{12}) \end{bmatrix} \quad \text{(S24)}$$

We named matrix **T** the *coevolutionary matrix* because the pervasive role of reciprocal effects affecting all of the elements of matrix **T**. The role of reciprocal effects on trait evolution held for both simple and complex network structures because species are connected by direct or indirect interactions in any connected network. For example, in the linear network studied here (Fig. 1C), species 1 and species 3 do not interact. However, element t_{13}, which describes the effects of species 3 on species 1, was nonzero if the evolutionary effects of species 3 on species 2, q_{32}^*, and of species 2 on species 1, q_{21}^*, were nonzero. The evolutionary effect of species 3 on species 1 was indirect in the sense that the selective pressures of species 3 on species 2 changed the evolutionary consequences of the selection imposed by species 2 on species 1. Thus, the indirect effect was a consequence of pathways linking non-interacting species in the network.

The coevolutionary matrix strongly differed from the structure of selection imposed by direct interactions, as can be observed through from visual inspection (Fig. 2A). This difference was also illustrated by the matrix spectra of both matrices (Fig. S1).

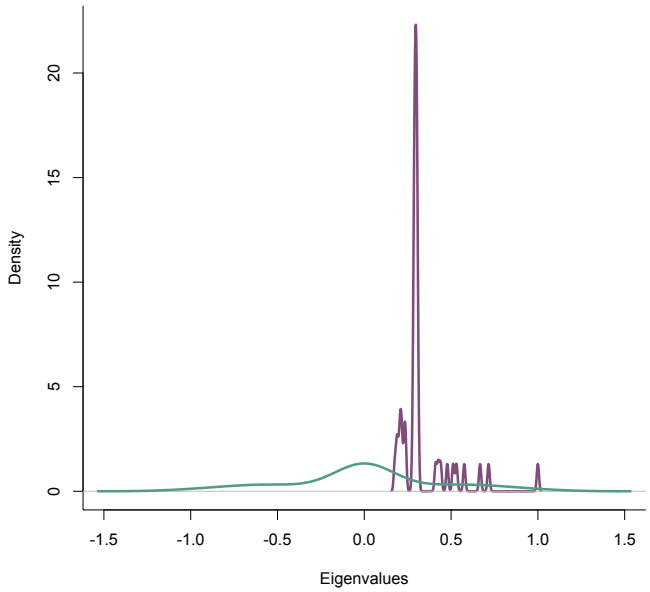

Figure S1. The matrix spectrum is the set of eigenvalues of a given matrix, which are represented by density functions. The set of eigenvalues provides information on the structure of the matrix; two matrices that strongly differ in their spectra also strongly differ in their structure[40]. The matrix spectra show how the structure of selection imposed by direct interactions (green curve) strongly differed from the coevolutionary matrix (purple curve), which contains the effects of interacting species and the indirect effects of non-interacting species on trait evolution. The simulation was parameterized with data on a seed dispersal network in Spain (network 45, Supplementary Table 1) and $\langle m \rangle = 0.7 \pm 0.01$. Similar results held for the other mutualistic networks.

We performed an analytical approximation of the coevolutionary model to understand how the effects of interacting and non-interacting species in reshaping the adaptive peaks of the component species of the network were related to the structure of selection imposed by direct interactions and its indirect effects. This analytical approximation held for any network structure. We assumed that $\mathbf{Q}^*$ can be approximated by $\mathbf{Q}$. This assumption holds if trait values are near the equilibrium and/or if evolution does not strongly affect the evolutionary effects of mutualistic interactions on trait evolution. This assumption allowed us to compute the cascading evolutionary effects occurring in the network by means of powers of matrix $\mathbf{Q}$, in which $\mathbf{Q}^\zeta$ is the ζth-power of $\mathbf{Q}$. The matrix $\mathbf{Q}^\zeta$ has a direct network interpretation: If $\mathbf{Q}$ defines a weighted network – as in our case, where the weights represent the direct evolutionary

effects between interacting species – the elements of $\mathbf{Q}^{\zeta}$ describe the effects of all pathways of length ζ that connect pairs of species in the network. A pathway (or a walk) is any sequence of nodes (species) and links (interactions), which are distinct or indistinct, starting and ending with nodes. The pathway length, ζ, is the number of times that links (distinct or not) were used as part of the pathway. For example, q_{ij}^2 is an element of $\mathbf{Q^2}$ and $q_{ij}^2 > 0$ if there is at least one pathway of length two that connects species i and j with the form $q_{ik}q_{kj}$, where $q_{ik} > 0$, and $q_{kj} > 0$. Accordingly, q_{ij}^3 is a nonzero element of $\mathbf{Q^3}$ if there is at least one pathway with the form $q_{ik}q_{kl}q_{lj}$ in which $q_{ik} > 0$, $q_{kl} > 0$, and $q_{lj} > 0$, and so on.

Because the traits are under environmental selection, with $\sum_j^N q_{ij}^* < 1$ for any species i, the real component of the leading eigenvalue of $\mathbf{Q}$, $\lambda_{\mathbf{Q}}^1$, is bounded ($0 < \lambda_{\mathbf{Q}}^1 < 1$), and the following equality holds:

$$\mathbf{Q^0} + \mathbf{Q^1} + \mathbf{Q^2} + \mathbf{Q^3} + \cdots + \mathbf{Q}^{\infty} = \sum_{\zeta=0}^{\infty} \mathbf{Q}^{\zeta} = (\mathbf{I} - \mathbf{Q})^{-\mathbf{1}} \quad \text{(S25)}$$

where $\mathbf{Q^0} = \mathbf{I}$. Therefore, $(\mathbf{I} - \mathbf{Q})^{-\mathbf{1}}$ describes the sum of the effects of all coevolutionary pathways of all lengths connecting any pair of species in the network. The coevolutionary matrix $\mathbf{T} = (\mathbf{I} - \mathbf{Q})^{-\mathbf{1}}\boldsymbol{\Psi}$ combines in a single descriptor the effects of interacting species, the indirect effects of non-interacting species, and the relative relevance of environmental selection as a driver of phenotypic evolution ($\mathbf{Q^0\Psi}$). Note that the equation $\mathbf{Z}^* = (\mathbf{I} - \mathbf{Q})^{-\mathbf{1}}\boldsymbol{\Psi\Theta}$ (eq. S8) is similar to the equation describing the Katz centrality, $\mathbf{K} = (\mathbf{I} - \vartheta\mathbf{W})^{-\mathbf{1}}\mathbf{1}$, (see Ref. 41) in which $\mathbf{1}$ is an all-ones vector, $\mathbf{W}$ is an adjacency matrix and ϑ is a scalar $0 < \vartheta < \frac{1}{\lambda_{\mathbf{W}}}$, in which $\lambda_{\mathbf{W}}$ is the leading eigenvalue of $\mathbf{W}$. The similarity is a consequence of both equations being based in a geometric series of matrices. Thus, the trait values in the equilibrium in the coevolutionary model are proportional to Katz centralities if (i) all values of mutualistic selection are identical to all species, (ii) $\mathbf{Q} = \vartheta\mathbf{W}$, and (iii) all elements of the vector $\boldsymbol{\Psi\Theta}$ are identical.

1.3. Sensitivity analysis of the coevolutionary matrix

We used analytical approximations and numerical simulations to study how different multiple model assumptions affect the emergence of the coevolutionary matrix,

$\mathbf{T}$, through the relationship $\mathbf{Z}^* = \mathbf{T\Theta}$.

Environmental selection: The equality $\mathbf{Z}^* = \mathbf{T\Theta}$ holds only if $m_i < 1$ for any given species i in the network. If there is no environmental selection, $m_i = 1$, the trait values depend on the initial condition and network structure. In this scenario, if there are pathways connecting all pairs of species in the network, then all species traits converge to the same trait value at the equilibrium, Z^*. For large networks, this trait value at equilibrium was defined as $Z^* = \langle Z^0 \rangle + \varepsilon_s$, where $\langle Z^0 \rangle$ is the average of the mean trait values for all species at $t = 0$, and ε_s is the effect of the network structure on shaping the coevolutionary dynamics ($\varepsilon_s = 0.68 \pm 0.54$, estimated using a set of numerical simulations (simulation parameters: n = 10^2 simulations per empirical network, 75 empirical networks; $\langle \varphi \rangle = 0.2 \pm 0.01$, $m_i = 1$ for any species i). Thus, phenotypes at equilibrium were not related to environmental optima. If the network is formed by disconnected groups of interacting species (components), then this result holds for each group of interacting species. Therefore, the coevolutionary matrix $\mathbf{T}$ emerges only in the scenario in which traits affecting mutualisms are also affected by other selective pressures.

Fixed environmental and mutualistic selection: We assumed that the proportional contributions of mutualistic selection and environmental selection to the selection gradient were fixed at m_i and $1 - m_i$, respectively. However, it is likely that the relative contributions of selective pressures imposed by mutualisms and the environment vary with the phenotypic distance of the population from alternative adaptive peaks. For example, if a population has diverged too far from the trait value favored by environmental selection, one might expect that the environment would increase in importance as a source of selective pressures. We explored the consequences of violating the assumption of fixed contributions of environmental and mutualistic selection on the emergence of the coevolutionary matrix.

We developed an alternative version of the model in which the strength of mutualistic selection, m_i varied with time, decaying with the distance between the current mean trait value of a population and the trait value favored by environmental selection, θ_i, in such way that $m_i^t = e^{-c\left(Z_i^{(t)} - \theta_i\right)^2}$, where c is a scaling constant. In this version of the model, environmental selection was defined as $1 - e^{-c\left(Z_i^{(t)} - \theta_i\right)^2}$. As in

section 1.2, we tested whether the asymptotic trait values of the simulations, Z^*, were reproduced by the analytical prediction, $\mathbf{Z}^E = (\mathbf{I} - \mathbf{Q})^{-1}\mathbf{\Psi\Theta}$. We performed a new set of numerical simulations (simulation parameters: n = 10^2 simulations per empirical network, 75 empirical networks; $\langle\varphi\rangle = 0.2 \pm 0.01$, $\theta_i = U[0,10], c = 1$). We used $\mathbf{Q} = \mathbf{Q}^*$ and $\mathbf{\Psi} = \mathbf{\Psi}^*$ to compute $\mathbf{Z}^E$. $\mathbf{\Psi}^*$ is an NxN diagonal matrix in which $\psi_{ii} = 1 - m_i^*$ for any species i, and m_i^* is the level of mutualistic selection at equilibrium. We compared the mean absolute difference between $\mathbf{Z}^*$ and $\mathbf{Z}^E$ to investigate whether the analytical prediction holds if environmental selection and mutualistic selection were not fixed. The simulations suggested that the assumption of a fixed contribution of mutualism and environment to selection is not crucial for the emergence of the coevolutionary matrix (the mean absolute difference between $\mathbf{Z}^*$ and $\mathbf{Z}^E$ was $8.44\times10^{-5} \pm 4.33\times10^{-4}$).

Evolutionary effects of mutualisms: We showed in section 1.2 that the equality $\mathbf{Z}^* = \mathbf{T\Theta}$ held for fixed evolutionary effects, $q_{ij}^t = q_{ij}$ (analytical result), and for evolutionary dependences that evolve across time following equation 1 (numerical simulations). We also performed an additional set of simulations (parameters: n = 10^2 simulations per empirical network, 75 empirical networks; $\langle\varphi\rangle = 0.2 \pm 0.01$, $\theta_i = U[0,10]$, and $\langle m\rangle = 0.7 \pm 0.01$) in which we changed the definition of q_{ij}^t to:

$$q_{ij}^{(t)} = m_i \frac{a_{ij}\left|Z_j^{(t)} - Z_i^{(t)}\right|^{-1}}{\sum_{k=1,k\neq i}^{N} a_{ik}\left|Z_k^{(t)} - Z_i^{(t)}\right|^{-1}} \quad \text{(S24)}$$

We compared the mean absolute difference between $\mathbf{Z}^*$ and $\mathbf{Z}^E$ to investigate whether the analytical prediction for trait values ($\mathbf{Z}^E$) reproduces the results of numerical simulations $\mathbf{Z}^*$ under this alternative definition of evolutionary effects. We estimated $\mathbf{Z}^E$ as $\mathbf{Z}^E = (\mathbf{I} - \mathbf{Q}^*)^{-1}\mathbf{\Psi\Theta}$. The simulations corroborated the performance of the analytical approximation. The mean absolute difference between $\mathbf{Z}^*$ and $\mathbf{Z}^E$ was $1.2\times10^{-3} \pm 6.0\times10^{-3}$(mean $\pm$ SD). Hence, the equality $\mathbf{Z}^* = \mathbf{T\Theta}$ holds whether assuming fixed evolutionary effects (analytical approximation), time-dependent Gaussian effects of trait matching on evolutionary effects (baseline simulations), or time-dependent linear effects of trait matching (these simulations). Therefore, $\mathbf{Z}^* = \mathbf{T\Theta}$ was not a consequence of the particular functional form chosen for the evolutionary effects in the baseline simulations.

Barrier effects of other traits: We modeled the implicit effects of other traits as barrier effects that allow the interactions to occur, $a_{ij} = 1$, or prevent the interaction from occurring, $a_{ij} = 0$. However, in addition to barrier effects, traits might exert quantitative effects on selection that affect the evolution of other traits, such as Z. For example, in plant-frugivore interactions, different color patterns can attract distinct frugivores at different rates[42], thereby affecting fruit consumption and selection on other fruit traits. Quantitative effects can be modeled using matrix **A** and allowing a_{ij} to assume any quantitative (and positive) value. Equation 2 (main text), however, guarantees that the elements of **Q** are bounded between zero and the level of mutualistic selection of each species. Under the assumption of environmental selection, all eigenvalues of **Q** are less than one, implying that $\mathbf{Z}^* = \mathbf{T\Theta}$ holds even if the elements of **A** are quantitative. This analysis, however, did not address the problem of the changes in the barrier effects across time. Therefore, we subsequently investigated the scenarios in which the barrier effects leading to forbidden links are not fixed.

Fixed forbidden links: We assumed that forbidden links are fixed across time, which allowed us to explore the effects of network structure on coevolutionary dynamics. This assumption implies that other traits that prevent the interaction from occurring are evolving at slower rates than Z. However, this model decision implies that no interaction rewiring occurs. Mismatched interactions might become functionally zero, $q_{ij}^{(t)} \to 0$, where species i has alternative partners. Nevertheless, no novel interaction emerged, and specialists interacted only with their partners, regardless of the level of mismatching in the interaction.

We explored whether the assumption of fixed forbidden links is needed for the emergence of the coevolutionary matrix by simulating an alternative version of our coevolutionary model with a single modification: at each time step, there was a probability that one species would show an interaction switch due to adaptive rewiring[43]. The interaction switch simulated, at the population level, the effects of the propagation of new traits within the population. These traits were not modeled explicitly, but they allowed partner assemblages of species to evolve, changing forbidden links. We simulated the interaction switch using an algorithm divided into five steps.

(1) At each time step, there was a probability p_r of one species in the network

switching interactions.

(2) If so, species *i* was randomly selected.

(3) We set $a_{ij} = 0$ and $q_{ij}^{(t)} = 0$ if the interaction with species *j* had the smallest evolutionary effect on species *i* among all interacting partners of *i*.

(4) We then set $a_{ik} = 1$, $q_{ik}^{(t)} = m_i a_{ik} \frac{e^{-\alpha(Z_k - Z_i)^2}}{\sum_{r,r\neq i}^{N} a_{ir} e^{-\alpha(Z_r - Z_i)^2}}$, if

(i) species *k* was a potential partner of species *i*, e.g., if species *i* was a fruiting plant, and species *k* was a frugivore;

(ii) there was a forbidden link before the interaction switch that prevented the interaction between species *k* and species *i* from occurring, $a_{ik} = 0$;

(iii) $|Z_k - Z_i|$ was the smallest trait difference between Z_i and all potential partners of *i* that did not currently interact with species *i*;

(iv) $|Z_k - Z_i| < |Z_j - Z_i|$, if this inequality did not hold, then no rewiring occurred; and

(v) if rewiring occurred, and $\sum_{s=1}^{N} a_{js} = 0$, then species *j* was reconnected to the network by selecting from among all potential partners the one for which the trait difference was minimal, as in item *(iii)* of step (4).

We explored whether the definition of the coevolutionary matrix held in simulations that did not assume fixed forbidden links. We tested three distinct values of p_r, $p_r = \{10^{-2}, 10^{-3}, 10^{-4}\}$. We performed *100* simulations for each combination of p_r and empirical network (parameters: n = 10^2 simulations per empirical network, 75 empirical networks; $\langle\varphi\rangle = 0.2 \pm 0.01$, $\theta_i = U[0,10]$, and $\langle m\rangle = 0.7 \pm 0.01$). We computed the mean absolute difference between $\mathbf{Z}^*$ and $\mathbf{Z}^E$ and estimated $\mathbf{Z}^E$ as $\mathbf{Z}^E = (\mathbf{I} - \mathbf{Q}^*)^{-1}\mathbf{\Psi\Theta}$. Then, we computed the mean value of the mean absolute difference between $\mathbf{Z}^*$ and $\mathbf{Z}^E$ for all simulations using the same value p_r and empirical network *v*. The simulations corroborated the performance of the analytical approximation even without assuming fixed forbidden links: $\langle d_{p_r,v}\rangle$ was always minimal [$1.4\times10^{-5} \pm 4.9\times10^{-7}$ (mean $\pm$ SD)] regardless of the value of p_r. Thus, the equality $\mathbf{Z}^* = \mathbf{T\Theta}$ held regardless of the assumption of fixed forbidden links.

Fitness function: There are multiple ways of modeling trait matching and its fitness consequences. For example, Nuismer *et al.*[44] explicitly modeled the fitness function of

each individual, whereas our approach modeled the selection gradients. Combining individual-based modeling and analytical approximation, Nuismer *et al.*[14] modeled how the fitness of an individual animal with phenotype Z_{ih} varied with the phenotype Z_{jm} of a single potential plant partner and environmental selection as:

$$W_{ih_{(Z_{ih})}} = e^{-\gamma_i (Z_{ih}-\theta_i)^2}\left[1+\xi_i e^{-\alpha\left(Z_{ih}-Z_{jk}\right)^2}\right] \quad \text{(S26)}$$

where $W_{ih_{(Z_{ih})}}$ is the fitness of individual h of species i, Z_{ih} is the phenotype of individual h, Z_{jk} is the phenotype of individual k of species j, γ_i and α are scaling constants that describe the strength of environmental and mutualistic selection, and ξ_i measures the relevance of mutualisms for the fitness of species i. Under the assumption of weak selection favoring trait matching and assuming, without lack of generality, that species i is an animal species in a plant-animal mutualistic network, equation S26 led to the following equation, which describes the change in the mean trait value of species i at each time step:

$$\Delta Z_i = \sigma^2_{G_{Z_i}}\left[\frac{2\alpha\xi_i}{1+\xi_i}\left(\sum_{j=1}^{N_P} f_j Z_j - Z_i\right) + 2\gamma_A\left(\theta_{A,i} - Z_i\right)\right] + \delta_i \quad \text{(S27)}$$

where $\sigma^2_{G_{Z_i}}$ is the additive genetic variance of trait Z of species i, f_j is the relative frequency of individuals of plant species j among all plant species, $\gamma_i = \gamma_A$ for any species i, and δ_i is the change in the mean trait of species i due to genetic drift. The above model assumes that any individual of any animal species can interact with any individual of any plant species, i.e., there are no forbidden links. By incorporating forbidden links due to the effects of other traits, and under the simplifying assumptions that $\gamma_A = \gamma$ for all of the species in the network, we derived the equation describing the mean change of a given species i in the network:

$$\Delta Z_i = \sigma^2_{G_{Z_i}}\left[\frac{2\alpha\xi_i}{1+\xi_i}\left(\sum_{j=1}^{N} a_{ij} f_j Z_j - Z_i\right) + 2\gamma\left(\theta_i - Z_i\right)\right] + \delta_i \quad \text{(S28)}$$

where a_{ij} is an element of the adjacency matrix, and $a_{ij} = 0$ if species i and j are from distinct sets (animals or plants, for example) or if there is a forbidden link. Under the notation of our model,

$$Z_i^{(t+1)} = Z_i^{(t)} + \sigma^2_{G_{Z_i}}\left[\frac{2\alpha\xi_i}{1+\xi_i}\left(\sum_{j=1}^{N} a_{ij} f_j Z_j^{(t)} - Z_i^{(t)}\right) + 2\gamma\left(\theta_i - Z_i^{(t)}\right)\right] + \delta_i \quad \text{(S29)}$$

Noting that $\sum_{j=1}^{N} a_{ij} f_j = 1$,

$$Z_i^{(t+1)} = Z_i^{(t)} + \sigma_{G_{Z_i}}^2 \left\{ \left[\sum_{j=1}^{N} \frac{2\alpha\xi_i}{1+\xi_i} a_{ij} f_j \left(Z_j^{(t)} - Z_i^{(t)} \right) \right] + 2\gamma \left(\theta_i - Z_i^{(t)} \right) \right\} + \delta_i \quad \text{(S30)}$$

Equation S30 led to equation 1 in the main text, assuming the parameter equalities $2\gamma = \varrho_i\left(1 - \sum_{j,j\neq i}^{N} q_{ij}^t\right)$ and $\frac{2\alpha\xi_i}{1+\xi_i} a_{ij} f_j = \varrho_i q_{ij}^t$ and that genetic drift had a negligible effect, $\delta_i = 0$:

$$Z_i^{(t+1)} = Z_i^{(t)} + \varphi_i \left[\sum_{j,j\neq i}^{N} q_{ij}^{(t)} \left(Z_j^{(t)} - Z_i^{(t)} \right) + \left(1 - \sum_{j,j\neq i}^{N} q_{ij}^{(t)} \right) \left(\theta_i - Z_i^{(t)} \right) \right] \quad (1),$$

By mapping a different fitness function than the one used to derive the coevolutionary matrix, we showed that the coevolutionary matrix is not a consequence of the specific way we modeled the fitness consequences of trait matching to mutualisms. Instead, the coevolutionary matrix emerged under different modeling approaches.

Compound parameter φ_i : The compound parameter φ_i controls how rapidly phenotypes change in response to the selection gradient. In our analytical approximation, the φ_i values did not affect the emergence of the coevolutionary matrix. However, this result is a consequence of assuming that the matrix $\mathbf{Q}$ is fixed. In the numerical simulations of our coevolutionary model, q_{ij}^t evolved with trait matching. If there were more than two species (see section 2 for the pairwise scenario), the φ_i values affected the specific trait values at the equilibrium and, consequently, the elements of $\mathbf{Q}$. However, changes in the specific values of $\mathbf{Q}$ invalidate only the relationships $\mathbf{T} = (\mathbf{I} - \mathbf{Q})^{-1}\boldsymbol{\Psi}$ and $\mathbf{Z}^* = \mathbf{T}\boldsymbol{\Theta}$ if the leading eigenvalue of $\mathbf{Q}$ is equal to one. Because the φ_i values did not affect the eigenvalues of $\mathbf{Q}$, the relationships supporting the coevolutionary matrix held regardless of the values of φ_i.

2. Indirect effects and different types of mutualisms

We first computed the mean contribution of indirect effects to trait evolution for each combination of empirical network and level of mutualism selection, which varied from 0.2 to 0.9 (in increments of 0.1). We then fitted a general linear model (GLM) using JMP 9.0 to investigate whether types of mutualism vary in terms of the contribution of indirect effects to trait evolution. In this GLM, the response variable was the relative contribution of indirect effects, and the explanatory variables were the type of

mutualism (coded as six different types of mutualism, Fig. 3B) and the mean level of mutualistic selection. Although, we reported the *P*-values in the summary of the model's results, *P*-value estimates in numerical simulation studies do not provide much information[45], and we were more interested in the *F*-values and least-squares estimates. The higher the level of mutualistic selection, the higher was the contribution of indirect effects to the trait evolution (least squares estimate: 0.691 ± 0.01, mean $\pm$ SE, Supplementary Table 2). After controlling for the level of mutualistic selection, the relative contribution of indirect effects to trait evolution varied among the different types of mutualisms (Supplementary Table 2). We identified three groups of mutualistic networks that were statistically distinct when comparing the relative contribution of indirect effects to trait evolution (Tukey HSD test). The first group was formed by all of the multiple-partner interactions in the dataset: plant-seed disperser interactions (MLS estimate: 0.392 ± 0.005), plant-pollinator interactions (0.383 ± 0.004), cleaner-client interactions (0.377 ± 0.012), and plants that bear nectaries and protective ants (0.372 ± 0.010). The other two groups were formed by the other two types of intimate mutualism: anemone-anemonefish interactions (0.232 ± 0.006) and myrmecophytes and protective ants (0.178 ± 0.008).

The mutualisms varied markedly in their species richness. We tested whether the differences in the contribution of indirect effects to trait evolution held after controlling for differences in species richness. We performed a second GLM using species richness as an additional factor. We detected a small effect of species richness on the contribution of indirect effects to coevolutionary dynamics (MLS estimate: $6.35\times10^{-4} \pm 6.46\times10^{-5}$, Supplementary Table 3), but after controlling for the effects of species richness, the same patterns held. The level of mutualistic selection positively affected the contribution of indirect effects to trait evolution (MLS estimate: 0.691 ± 0.10, Supplementary Table 3). Accordingly, after controlling for the effects of species richness and the level of mutualistic selection, mutualisms could be grouped into the same three statistically distinct groups (Tukey's HSD test): (1) multiple-partner mutualisms: plant-seed disperser interactions (MLS estimate: 0.387 ± 0.004), plant-pollinator interactions (0.371 ± 0.004), cleaner-client interactions (0.383 ± 0.012), and plants that bear nectaries and protective ants (0.362 ± 0.009), (2) anemone-anemonefish interactions (0.261 ± 0.007), and (3) myrmecophytes and protective ants (0.199 ± 0.007).

We used a subset of the empirical networks to verify the result that multiple-partner mutualisms show higher contributions of indirect effects to trait evolution than intimate mutualisms. This subset was formed by 38 networks of three distinct mutualisms (plant-seed disperser, n = 13 networks; plant-pollinator, n = 18 networks; and myrmecophyte-ant interactions, n = 7 networks) for which we had empirical quantitative information on the ecological dependences among species. We did not run simulations of the coevolutionary model in this analysis. Instead, we assumed that the level of direct selection imposed by a given partner was a function of the frequency of the interactions and the level of mutualistic selection, m_i:

$$q_{ij} = m_i \frac{v_{ij}}{\sum_{k=1}^{N} v_{ik}}, \qquad \text{(S.31)}$$

where v_{ij} is the number of recorded interaction events between individuals of species i and j in the empirical studies. Because $0 < m_i < 1$ for any species i, all eigenvalues of **Q** were less than one, and consequently, **T**-matrix could be estimated using equation S18. In a given simulation, we randomly sampled m_i from a normal distribution, $\langle m \rangle \pm 0.01$ for any species i in the network, and then estimated **T**-matrix using equations S8 and S31. Subsequently, we computed the contribution of indirect effects to trait evolution using **T**. We repeated this algorithm 100 times for each combination of mean mutualistic selection, $\langle m \rangle$, and network. We varied the mean level of mutualistic selection, $\langle m \rangle$, from 0.2 to 0.9 (in increments of 0.1), yielding 800 simulations per network. We then computed the mean contribution of indirect effects per network using this ensemble of 800 networks. We used this mean estimate as the response variable in a GLM, with the type of mutualism used as the explanatory variable. Again, multiple-partner mutualisms showed higher contributions of indirect effects (MLS estimates: plant-seed disperser interactions = 0.399 ± 0.011 and plant-pollinator interactions = 0.391 ± 0.009) than intimate mutualisms (interactions among myrmecophytes and protective ants $=0.183 \pm 0.015$, $F_{2,35} = 83.70$, $P < 0.0001$).

3. Indirect effects and network structure

Our analysis showed that the first principal component (PC1) was positively associated with the contribution of indirect effects to coevolutionary dynamics (Fig. 3C). For our baseline simulations, we computed the mean contribution of indirect effects per

network (Fig. 3). We then explored the effects of each of network metric on the contribution of indirect effects to trait evolution using simple linear regressions. We corroborated the results that the contribution of indirect effects to trait evolution was positively associated with species richness and nestedness and negatively associated with connectance and modularity (Supplementary Table 5).

We then performed an analytical approximation to investigate how network structural pattern affects the relative contributions of interacting and non-interacting species to trait evolution in mutualistic networks. We focused on how indirect effects affect the trait evolution of an animal species *i* in a plant-animal mutualistic network. However, the results can be directly applied to any species in a mutualistic network with a bipartite structure. Our analytical results and numerical simulations suggested that the effects of mutualistic species on evolution and coevolution in the network can be described by direct and indirect evolutionary effects, as described by equation S25:

$$(\mathbf{I}-\mathbf{Q})^{-1}=\mathbf{Q}^{0}+\mathbf{Q}^{1}+\mathbf{Q}^{2}+\mathbf{Q}^{3}+\cdots+\mathbf{Q}^{\infty}=\sum_{\zeta=0}^{\infty}\mathbf{Q}^{\zeta} \quad \text{(S32)}$$

We then analyzed how the network structure can increase the contribution of indirect effects to the trait evolution of species *i*. We made the following simplifying assumptions: $m_i = m$ for all species in the network, and N_A and N_B are large. We computed the effect of species *j* on species *i* through all of the pathways connecting species *j* to species *i*:

$$t_{ij}=(1-m)\sum_{\zeta=0}^{\infty}q_{ij}^{\zeta} \quad \text{(S33)}$$

We approximated q_{ij}^{ζ} by noting that on average, the expected effect of a given pathway is $\langle q\rangle^{\zeta}$, where $\langle q\rangle$ is the mean evolutionary effect of a mutualistic interaction. Thus, the expected number of pathways of length ζ connecting species *i* to *j* as n_{ij}^{ζ} is:

$$q_{ij}^{\zeta}=n_{ij}^{\zeta}\langle q\rangle^{\zeta} \quad \text{(S34)}$$

The expected number of pathways connecting species in a network depends on the structure of the adjacency matrix **A**. The number of pathways connecting species in a network increases with the pathway length; this phenomenon is called pathway proliferation[46]:

$$n_{ij}^{\zeta}=a{\lambda_A}^{\zeta} \quad \text{(S35)}$$

where λ_A is the leading eigenvalue of the binary adjacency matrix and depends on network structure (see below), and $a = \frac{L}{\lambda_A N_A N_B}$. Substituting S35 into S34 yields:

$$q_{ij}^{\zeta} = \frac{L}{\lambda_A N_A N_B}(\lambda_A \langle q \rangle)^{\zeta} \quad \text{(S36)}$$

In our simulations, the effects of pathways on trait evolution converged, implying that increasing the number of pathways, ${\lambda_A}^{\zeta}$, did not compensate for the decay of evolutionary effects with pathway length, $\langle q \rangle^{\zeta}$. In our mean-field analytical approximation, this convergence implied:

$$\lambda_A \langle q \rangle < 1. \quad \text{(S37)}$$

In this mean-field analytical approximation, this condition for convergence holds if mutualistic selection is weak or if the network is sufficiently connected (see section 3.1). We searched for differences in the contributions made by other species in the network to the trait evolution of animal species *i*. To do so, we focused on the contributions of two plant species: plant species *j* interacts with animal species *i*, whereas plant species *k* does not interact with animal species *i*. Because the structure is bipartite, only odd pathways, i.e., pathways with an odd number of links, would contribute to the evolutionary effects of plant species on any given animal species. Under the assumptions $m_i = m$ and $\psi_{ii} = 1 - m$ for any species *i*, the expected effect of a given plant species *j* that directly interacts with species *i* on species *i* is:

$$t_{ij} = (1-m)\frac{L}{\lambda_A N_A N_B}\sum_{i=1}^{\infty} {\lambda_A}^{2i-1}\langle q \rangle^{2i-1} \quad \text{(S38)}$$

As a consequence of $\lambda_A \langle q \rangle < 1$,

$$t_{ij} = (1-m)\frac{L}{\lambda_A N_A N_B}\left(\frac{\lambda_A \langle q \rangle}{1-{\lambda_A}^2 \langle q \rangle^2}\right) \quad \text{(S39)}$$

Accordingly, the expected effect of a given plant species *k* that does not directly interact with species *i* is:

$$t_{ik} = (1-m)\frac{L}{\lambda_A N_A N_B}\sum_{i=2}^{\infty} {\lambda_A}^{2i-1}\langle q \rangle^{2i-1} \quad \text{(S40a)}$$

$$t_{ik} = (1-m)\frac{L}{\lambda_A N_A N_B}\left(\frac{\lambda_A \langle q \rangle}{1-{\lambda_A}^2 \langle q \rangle^2} - \lambda_A \langle q \rangle\right) \quad \text{(S40b)}$$

We explored how the differences between t_{ij} and t_{ik} vary with λ_A. We computed the ratio between the two contributions:

$$\frac{t_{ik}}{t_{ij}} = {\lambda_A}^2 \langle q \rangle^2 \quad \text{(S41)}$$

For small leading eigenvalues, the contribution of a given plant species *j* that interacts with species *i* to the trait evolution of species *i* is much higher than the contribution of a plant species *k* that does not interact with species *i*. As the leading eigenvalue increases, the ratio between the contributions of interacting species *j* and non-interacting species *k* gets closer to one, and both species contribute similarly to the evolution of species *i*. Therefore, as the leading eigenvalue increases, the contributions of interacting and non-interacting species becomes increasingly similar. Thus, the leading eigenvalue, which is the rate of pathway proliferation[46], may contribute to trait evolution.

We next explored how network properties favor or constrain the number of pathways in a given network by increasing or decreasing the leading eigenvalue. We reviewed the results of spectral graph theory relating λ_A^1 to species richness, connectance, modularity, and nestedness to understand why species richness and nestedness favor indirect effects, whereas modularity decreases the role of indirect effects. The upper boundary for the leading eigenvalue of a bipartite graph is:

$$\lambda_A^1 \leq \sqrt{L} \quad \text{(S42)}$$

The number of links in a bipartite graph is related to its species richness and connectance:

$$L = N_A N_B C \quad \text{(S43)}$$

where C is the connectance, and $N_A(N_B)$ is the species richness of set A (B). Combining S42 and S43 yields:

$$\lambda_A^1 \leq \sqrt{N_A N_B C} \quad \text{(S44)}$$

Therefore, the upper bound on the leading eigenvalue is positively affected by increasing species richness and/or connectance. Because the contribution of indirect effects is affected by the leading eigenvalue of matrix **A**, this result explains the positive association between species richness and the contribution of indirect effects to the trait evolution observed in the numerical simulations. However, the incongruence between the results of the principal component analysis (PCA) and spectral graph theory on the role of connectance in the contribution of indirect effects suggests that the effects of connectance on the upper bound values of leading eigenvalues do not affect the amount of indirect effects.

The level of nestedness of a network is the degree to which the interactions of a given species i with k_i interactions are a proper subset of the interactions of a species j with $k_j > k_i$ interactions. The spectral properties of nestedness in ecological networks were explored using the spectral properties of double-nested graphs[47]. Although the concept of perfect nestedness in ecological systems is distinct from the concept of double-nested graphs[30,48-50], double-nested graphs provide a useful connection between nestedness and spectral graph theory. For fixed values of species richness and connectance, the graph with the largest λ_A^1 is a double-nested graph[47]. Therefore, after controlling for the effects of species richness and connectance, greater nestedness values should result in higher contributions of non-interacting species. In fact, we detected a positive relationship between nestedness, measured using an independent index — the nestedness metric based on overlap and decreasing fill (NODF)—, and the relative contribution to trait evolution.

The level of modularity is the level to which the species of a network are arranged as semi-isolated groups of interacting nodes called modules. Multiple modules with just a few interactions between modules characterize a network with a high level of modularity. As a consequence, connectance is often small in modular networks, resulting in a reduction in the upper bound of λ_A^1. Moreover, the formation of semi-independent modules within networks reduces the largest eigenvalue of the network. For example, consider the limiting case in which the network is formed by M isolated components, in which there is no pathway connecting nodes in two distinct components. Let us define $\mathbf{A_b}$ as a submatrix of $\mathbf{A}$, describing a component b. In this scenario, $\lambda_A^1 = \max_b \lambda_{A_b}$, where $\max_b \lambda_{A_b}$ is the largest among the leading eigenvalues of all submatrices defining the components of $\mathbf{A}$[46]. If we assume the network has at least two components, then the number of interactions of either component is smaller than the number of interactions of the network. Therefore,

$$\lambda_A^1 = \max_b \lambda_{A_b} < \sqrt{L} \qquad \text{(S45)}$$

As a result, modularity reduces the leading eigenvalue and, consequently, the contribution of non-interacting species.

3.1. Conditions for the mean-field approximation of coevolutionary pathways

We verified the conditions under which the assumption $\lambda_A\langle q\rangle < 1$ holds in our analytical approximation. We made the simplifying assumption that $N_A = N_B = N_m$. The expected direct evolutionary effect of a given interaction, $\langle q\rangle$, can be defined as $\langle q\rangle = m\frac{1}{\langle k\rangle} = m\frac{N_m}{L}$. The total number of interactions in this approximation was $L = CN_m{}^2$. We used these equations to rewrite $\lambda_A\langle q\rangle < 1$ as follows:

$$\lambda_A m\frac{N_m}{L} < 1 \quad \text{(S46a)}$$

$$\lambda_A < \frac{L}{mN_m} \quad \text{(S46b)}$$

We explored the limiting case in which the eigenvalue is maximal in a bipartite graph, $\lambda_A = \sqrt{L}$ (S42). Combining S42 and S46 yields:

$$\sqrt{L} < \frac{L}{mN_m} \quad \text{(S47a)}$$

$$N_m\sqrt{C} < \frac{CN_m{}^2}{mN_m} \quad \text{(S47b)}$$

$$m < \sqrt{C} \quad \text{(S47c)}$$

Therefore, our analytical approximation held if mutualistic selection, m, is sufficiently weak and/or the network connectance (C) is sufficiently large.

4. Environmental change simulation

We constructed a GLM addressing the relationships of indirect effects with the time-to-equilibrium of the coevolutionary dynamics and the amount of directional evolutionary change recorded in our simulations of environmental change. We estimated the contribution of indirect effects to coevolutionary dynamics as the least square estimates of the effect of network structure on the relative contribution of indirect effects after controlling for the level of mutualistic selection. Species richness affected the relative contribution of indirect effects to trait evolution (linear-log regression, slope = 0.10, $R^2 = 0.64$, $F_{1,73} = 129.47$, $P < 0.0001$) and the response variables (time-to-equilibrium: simple linear regression, slope = 0.80, $R^2 = 0.51$, $F_{1,73} = 75.72$, $P < 0.0001$; amount of directional change: linear-log regression, slope = -5.29×10^{-6}, $R^2 = 0.60$, $F_{1,73} = 107.83$, $P < 0.0001$). Hence, we performed an additional analysis controlling for the effects of species richness in both the explanatory and response variables. We used the residuals of the

relationship between species richness and all of the variables. We then performed simple linear regressions to investigate the relationship between the residuals of the least squares estimates and the residuals of the response variables. After controlling for the effects of species richness, the patterns reported in the main text held: Indirect effects were positively associated with time-to-equilibrium and negatively associated with the amount of evolutionary change (Supplementary Table 4).

In our baseline analyses, we changed the trait value favored by the environment to $\theta_i + \varepsilon_i$ for every species i. Because the change ε_i was randomly sampled from a uniform distribution [0,1], perturbation represents an increase in the trait values favored by environmental selection in all species. Thus, we also used one alternative perturbation scheme to determine whether our conclusions relating indirect effects to coevolutionary dynamics after perturbation were dependent on the perturbation scheme used. We ran an additional set of simulations following the same algorithm of the baseline perturbations with one difference: we sampled ε_i from a uniform distribution [-0.1,0.1]. In this new scheme, perturbations may increase or decrease the trait values favored by environmental selection. Despite the differences between perturbation schemes, the results are very similar to those of the baseline simulations. Indirect effects were positively associated with the time-to-equilibrium (log-linear regression, $R^2 = 0.61$, $F_{1,73} = 114.36$, $P < 0.001$) and the amount of directional change (simple linear regression, $R^2 = 0.83$, $F_{1,73} = 370.98$, $P < 0.001$). After controlling for the effects of species richness, the same patterns held when analyzing the residuals of the variables (time-to-equilibrium: linear regression, $R^2 = 0.23$, $F_{1,73} = 22.01$, $P < 0.001$; and amount of directional change: simple linear regression, $R^2 = 0.44$, $F_{1,73} = 57.49$, $P < 0.001$).

References

31. McQuaid, C. F. & Britton, N. F. Network dynamics contribute to structure: nestedness in mutualistic networks. *Bull. Math. Biol.* **75**, 2372-2388 (2013).
32. Loeuille, N. Influence of evolution on the stability of ecological communities. *Ecol. Lett.* **13**, 1536-1545 (2010).
33. Andreazzi, C. S., Thompson, J. N. & Guimarães, P. R. Network structure and selection asymmetry drive coevolution in species-rich antagonistic interactions. *Am. Nat.* **190**, 99-115 (2017).

34. Kauffman, S. A. & Johnsen, S. Coevolution to the edge of chaos: coupled fitness landscapes, poised states, and coevolutionary avalanches. *J. Theor. Biol.* **149**, 467-505 (1991).

35. Melo, D., Porto, A., Cheverud, J. M. & Marroig, G. Modularity: genes, development, and evolution. *Annu. Rev. Ecol. Evol. Syst.* **47**, 463-486 (2016).

36. Valido, A., Schaefer, H. M. & Jordano, P. Colour, design and reward: phenotypic integration of fleshy fruit displays. *J. Evol. Biol.* **24**, 751-760 (2011).

37. Herrera, C. M. Vertebrate-dispersed plants: why they don't behave the way they should, in *Frugivores and Seed Dispersal* (ed. Estrada, A, & Fleming, T) 5-18 (Springer, 1986).

38. Lande, R. Natural selection and random genetic drift in phenotypic evolution. *Evolution* **30**, 314-334 (1976).

39. Jordano, P., Bascompte, J. & Olesen, J. M. Invariant properties in coevolutionary networks of plant-animal interactions. *Ecol. Lett.* **6**, 69-81 (2003).

40. Lemos-Costa, P., Pires, M. M., Araújo, M. S., de Aguiar, M. A. M. & Guimarães, P. R. Network analyses support the role of prey preferences in shaping resource use patterns within five animal populations. *Oikos* 125, 492-501 (2016).

41. Newman, M. *Networks: An Introduction* (Oxford University Press, 2010).

42. Cazetta, E., Schaefer, H. M. & Galetti, M. Why are fruits colorful? The relative importance of achromatic and chromatic contrasts for detection by birds. *Evol. Ecol.* **23**, 233-244 (2009).

43. Suweis, S., Simini, F., Banavar, J. R. & Maritan, A. Emergence of structural and dynamical properties of ecological mutualistic networks. *Nature* **500**, 449–452 (2013).

44. Nuismer, S. L., Jordano, P. & Bascompte, J. Coevolution and the architecture of mutualistic networks. *Evolution* **67**, 338-354 (2013).

45. White, J. W., Rassweiler, A., Samhouri, J. F., Stier, A. C. & White, C. Ecologists should not use statistical significance tests to interpret simulation model results. *Oikos* **123**, 385-388 (2014).

46. Borrett, S. R., Fath, B. D. & Patten, B. C. Functional integration of ecological networks through pathway proliferation. *J. Theor. Biol.* **245**, 98-111 (2007).

47. Staniczenko, P. P., Kopp, J. C. & Allesina, S. The ghost of nestedness in ecological networks. *Nat. Comm.* **4**, 1391 (2013).

48. Atmar, W. & Patterson, B. D. The measure of order and disorder in the distribution of species in fragmented habitat. *Oecologia* **96**, 373-382 (1993).

49. Almeida-Neto, M., R. Guimarães Jr, P. & M. Lewinsohn, T. On nestedness analyses: rethinking matrix temperature and anti-nestedness. *Oikos* **116**, 716-722 (2007).

50. Ulrich, W., Almeida-Neto, M. & Gotelli, N. J. A consumer's guide to nestedness analysis. *Oikos* **118**, 3-17 (2009).

Supplementary Table 1. Empirical networks of distinct mutualisms used to parameterize the coevolutionary model and study indirect effects on coevolutionary dynamics. Each mutualism is identified by the two sets of species that interact; N_A = species richness of the first set of species (rows) (e.g., in anemone-anemonefish interactions, N_A refers to the species richness of anemones); N_B = species richness of the second set of the species (columns); binary = binary information on species interactions; quantitative = quantitative information on species interactions, C = connectance, Q_E = bipartite modularity index; N_E = nestedness (NODF); $\lambda_{\mathbf{A}}^1$ = leading eigenvalue of the adjacency matrix describing binary interactions; IWDB = dataset available for download at https://www.nceas.ucsb.edu/interactionweb/; Web-of-life = dataset available for download at http://www.web-of-life.es/; Rico-Gray = dataset kindly provided by Victor Rico-Gray; Izzo = dataset kindly provided by Thiago Izzo; Sazima = dataset kindly provided by Cristina and Ivan Sazima; Donatti = dataset kindly provided by Camila Donatti; Hasui = dataset kindly provided by Erica Hasui, Mariana Vidal, and Wesley Silva; Jordano = dataset provided by one of the authors (PJ).

#	*Mutualism*	*Country*	*Data*	N_A	N_B	C	Q_E	N_E	$\lambda_{\mathbf{A}}^1$	*Availability*
1	Anemone-Anemonefish	Indonesia	binary	4	4	0.44	0.39	62.5	2.22	IWDB[1]
2	Anemone-Anemonefish	Indonesia	binary	4	5	0.3	0.56	12.5	1.73	IWDB[1]
3	Anemone-Anemonefish	Indonesia	binary	4	4	0.44	0.39	29.17	2.03	IWDB[1]
4	Anemone-Anemonefish	Indonesia	binary	4	4	0.38	0.47	16.67	1.80	IWDB[1]
5	Anemone-Anemonefish	Indonesia	binary	5	5	0.32	0.48	22.5	1.99	IWDB[1]
6	Anemone-Anemonefish	Indonesia	binary	4	5	0.35	0.47	12.5	1.85	IWDB[1]
7	Anemone-Anemonefish	Indonesia	binary	6	5	0.33	0.44	38	2.39	IWDB[1]
8	Anemone-Anemonefish	Indonesia	binary	4	5	0.4	0.44	34.38	2.12	IWDB[1]
9	Anemone-Anemonefish	Indonesia	binary	3	4	0.5	0.33	22.22	1.85	IWDB[1]
10	Anemone-Anemonefish	Indonesia	binary	4	4	0.44	0.37	37.5	1.99	IWDB[1]
11	Anemone-Anemonefish	Indonesia	binary	5	3	0.47	0.41	38.46	2.00	IWDB[1]
12	Ant-Extrafloral nectar (EFN) plant	Australia	quantitative	41	51	0.14	0.31	43.51	11.34	IWDB[2]
13	Ant-EFN plant	Mexico	binary	10	38	0.25	0.36	39.17	6.65	Rico-Gray
14	Ant-EFN plant	Mexico	binary	28	99	0.1	0.47	40.59	10.64	Rico-Gray
15	Ant-EFN plant	Mexico	binary	5	12	0.22	0.75	2.63	2	Rico-Gray
16	Ant-EFN plant	Mexico	binary	13	46	0.21	0.45	35.55	7.54	Rico-Gray
17	Ant-myrmecophyte	Peru	binary	16	8	0.15	0.78	4.28	2.33	IWDB[3]
18	Ant-myrmecophyte	Brazil	quantitative	25	16	0.12	0.69	13.63	3.39	IWDB[4]
19	Ant-myrmecophyte	Brazil	quantitative	6	5	0.23	0.69	8	1.62	Izzo
20	Ant-myrmecophyte	Brazil	quantitative	9	7	0.17	0.78	7.02	1.62	Izzo
21	Ant-myrmecophyte	Brazil	quantitative	13	8	0.16	0.69	11.32	2.45	Izzo
22	Ant-myrmecophyte	Brazil	quantitative	8	7	0.16	0.79	0	1.73	Izzo

23	Ant-myrmecophyte	Brazil	quantitative	12	9	0.15	0.78	4.9	2.14	Izzo
24	Ant-myrmecophyte	Brazil	quantitative	10	8	0.15	0.78	4.11	1.85	Izzo
25	Cleaner-client	Brazil	binary	5	35	0.42	0.26	70.73	7.39	Sazima
26	Cleaner-client	Netherlands Antilles	binary	6	50	0.35	0.30	64.47	8.55	[5]
27	Cleaner-client	Virgin Islands	binary	4	32	0.41	0.36	46.30	5.85	[6]
28	Frugivore-plant	Australia	binary	7	72	0.28	0.33	51.67	9.62	Web-of-Life[7]
29	Frugivore-plant	Brazil	binary	46	45	0.13	0.42	27.8	9.93	Donatti
30	Frugivore-plant	Brazil	quantitative	29	35	0.14	0.38	35.49	7.73	Web-of-Life[8]
31	Frugivore-plant	Brazil	binary	44	42	0.09	0.46	17.15	6.38	Hasui
32	Frugivore-plant	Costa Rica	binary	40	169	0.1	0.40	32.87	15.06	Web-of-Life[9]
33	Frugivore-plant	Kenya	quantitative	88	33	0.14	0.31	34.58	14.05	IWDB[10]
34	Frugivore-plant	Malaysia	binary	61	25	0.34	0.21	58.86	17.88	Web-of-Life[11]
35	Frugivore-plant	Mexico	binary	27	5	0.64	0.18	67.34	8.12	Web-of-Life[12]
36	Frugivore-plant	Panamá	quantitative	19	4	0.43	0.35	48.29	4.56	IWDB[13]
37	Frugivore-plant	Panamá	quantitative	11	13	0.37	0.25	73.9	6	IWDB[13]
38	Frugivore-plant	Papua New Guinea	quantitative	9	31	0.43	0.22	67.66	9.01	Web-of-Life[14]
39	Frugivore-plant	Papua New Guinea	binary	32	29	0.07	0.65	11.21	4.04	Web-of-Life[15]
40	Frugivore-plant	Puerto Rico	quantitative	16	25	0.17	0.40	44.7	5.59	[16]
41	Frugivore-plant	Puerto Rico	quantitative	20	34	0.14	0.39	43.38	6.8	[16]
42	Frugivore-plant	Puerto Rico	quantitative	13	25	0.15	0.54	29.69	4.44	[16]
43	Frugivore-plant	Puerto Rico	quantitative	15	21	0.16	0.47	34.17	4.62	[16]
44	Frugivore-plant	Spain	quantitative	17	16	0.44	0.24	78.76	9.09	Jordano
45	Frugivore-plant	Spain	quantitative	33	25	0.18	0.33	58.98	8.65	[17]
46	Frugivore-plant	UK	quantitative	14	11	0.3	0.34	42.71	4.84	IWDB[18]
47	Frugivore-plant	USA	quantitative	21	7	0.34	0.32	50.98	5.38	Web-of-Life[19]
48	Pollinator-plant	Argentina	binary	45	21	0.09	0.62	18.02	4.86	Web-of-Life[20]
49	Pollinator-plant	Argentina	binary	72	23	0.08	0.59	22.88	6.74	Web-of-Life[20]
50	Pollinator-plant	Argentina	quantitative	29	10	0.15	0.54	29.54	4.62	IWDB[21]
51	Pollinator-plant	Argentina	quantitative	33	9	0.15	0.62	18.66	4.2	IWDB[21]
52	Pollinator-plant	Argentina	quantitative	29	10	0.14	0.58	26.31	4.67	IWDB[21]
53	Pollinator-plant	Argentina	quantitative	26	8	0.17	0.55	23.28	4.04	IWDB[21]
54	Pollinator-plant	Argentina	quantitative	27	8	0.22	0.50	30.31	4.52	IWDB[21]
55	Pollinator-plant	Australia	quantitative	85	40	0.08	0.42	19.31	8.7	Web-of-Life[22]

56	Pollinator-plant	Brazil	quantitative	13	13	0.42	0.23	84.93	7.29	Web-of-Life[23]
57	Pollinator-plant	Brazil	binary	25	51	0.15	0.32	46.36	9.39	[24]
58	Pollinator-plant	Canada	quantitative	102	12	0.14	0.49	30.78	8.7	Web-of-Life[25]
59	Pollinator-plant	Canada	binary	86	29	0.07	0.50	26.51	7.92	IWDB[26]
60	Pollinator-plant	Canada	quantitative	18	11	0.19	0.48	32.08	4.32	IWDB[27]
61	Pollinator-plant	Canada	quantitative	34	13	0.32	0.26	40.96	8.6	Web-of-Life[28]
62	Pollinator-plant	Chile	binary	101	87	0.04	0.52	14.72	9.02	[29]
63	Pollinator-plant	Chile	binary	64	42	0.07	0.53	16.26	6.82	[29]
64	Pollinator-plant	Chile	binary	28	41	0.08	0.61	19.25	4.9	[29]
65	Pollinator-plant	Mauritius	quantitative	100	58	0.09	0.31	34.35	15.09	IWDB[30]
66	Pollinator-plant	New Zealand	binary	60	18	0.11	0.56	13.94	5.23	Web-of-Life[32]
67	Pollinator-plant	Azores, Portugal	quantitative	12	10	0.25	0.44	35.96	3.68	IWDB[31]
68	Pollinator-plant	Canarias, Spain	quantitative	38	11	0.26	0.35	37.16	6.79	IWDB[33]
69	Pollinator-plant	Mauritius	quantitative	13	14	0.29	0.34	51.87	5.24	IWDB[31]
70	Pollinator-plant	South Africa	binary	56	9	0.20	0.44	35.49	7.04	Web-of-Life[34]
71	Pollinator-plant	Sweden	quantitative	118	24	0.085	0.51	15.39	7.91	Web-of-Life[35]
72	Pollinator-plant	UK	quantitative	61	17	0.14	0.38	52.27	8.57	Web-of-Life[36]
73	Pollinator-plant	UK	quantitative	36	16	0.15	0.44	35.66	6.12	Web-of-Life[36]
74	Pollinator-plant	USA	quantitative	33	7	0.28	0.36	56.66	6.41	Web-of-Life[37]
75	Pollinator-plant	Venezuela	binary	53	28	0.07	0.59	11.16	4.78	IWDB[38]

References

1. Ricciardi, F., Boyer, M. & Ollerton, J. Assemblage and interaction structure of the anemonefish-anemone mutualism across the Manado region of Sulawesi, Indonesia. *Environ. Biol. Fishes* **87**, 333-347 (2010).
2. Blüthgen, N., E Stork, N. & Fiedler, K. Bottom-up control and co-occurrence in complex communities: honeydew and nectar determine a rainforest ant mosaic. *Oikos* **106**, 344-358 (2004).
3. Davidson, D. W., Snelling, R. R. & Longino, J. T. Competition among ants for myrmecophytes and the significance of plant trichomes. *Biotropica*, 64-73 (1989).
4. Fonseca, C. R. & Ganade, G. Asymmetries, compartments and null interactions in an Amazonian ant-plant community. *J Anim Ecol*, 339-347 (1996).

5. Wicksten, M. Behaviour of cleaners and their client fishes at Bonaire, Netherlands Antilles. *J. Nat. Hist.* **32**, 13-30 (1998).
6. Johnson, W. S. & Ruben, P. Cleaning behavior of *Bodianus rufus*, *Thalassoma bifasciatum*, *Gobiosoma evelynae*, and *Periclimenes pedersoni* along a depth gradient at Salt River Submarine Canyon, St. Croix. *Environ. Biol. Fishes* **23**, 225-232 (1988).
7. Crome, F. The ecology of fruit pigeons in tropical Northern Queensland. *Wildl. Res.* **2**, 155-185 (1975).
8. Galetti, M. & Pizo, M. A. Fruit eating by birds in a forest fragment in southeastern Brazil. *Revista Brasileira de Ornitologia-Brazilian Journal of Ornithology* **4**, 9 (2013).
9. Wheelwright, N. T., Haber, W. A., Murray, K. G. & Guindon, C. Tropical fruit-eating birds and their food plants: a survey of a Costa Rican lower montane forest. *Biotropica*, 173-192 (1984).
10. Schleuning, M. *et al.* Specialization and interaction strength in a tropical plant–frugivore network differ among forest strata. *Ecology* **92**, 26-36 (2011).
11. Lambert, F. Fig-eating by birds in a Malaysian lowland rain forest. *J. Trop. Ecol.* **5**, 401-412 (1989).
12. Kantak, G. E. Observations on some fruit-eating birds in Mexico. *The Auk* **96**, 183-186 (1979).
13. Poulin, B., Wright, S. J., Lefebvre, G. & Calderón, O. Interspecific synchrony and asynchrony in the fruiting phenologies of congeneric bird-dispersed plants in Panama. *J. Trop. Ecol.* **15**, 213-227 (1999).
14. Beehler, B. Frugivory and polygamy in birds of paradise. *The Auk*, 1-12 (1983).
15. Mack, A. L. & Wright, D. D. Notes on occurrence and feeding of birds at Crater Mountain biological research station, Papua New Guinea. *Emu* **96**, 89-101 (1996).
16. Carlo, T. A., Collazo, J. A. & Groom, M. J. Avian fruit preferences across a Puerto Rican forested landscape: pattern consistency and implications for seed removal. *Oecologia* **134**, 119-131 (2003).
17. Rezende, E. L., Lavabre, J. E., Guimarães, P. R., Jordano, P. & Bascompte, J. Non-random coextinctions in phylogenetically structured mutualistic networks. *Nature* **448**, 925-928 (2007).
18. Sorensen, A. Interactions between birds and fruit in a temperate woodland. *Oecologia* **50**, 242-249 (1981).
19. Baird, J. W. The selection and use of fruit by birds in an eastern forest. *The Wilson Bulletin*, 63-73 (1980).

20. Medan, D. *et al.* Plant-pollinator relationships at two altitudes in the Andes of Mendoza, Argentina. *Arct. Antarct. Alp. Res.*, 233-241 (2002).
21. Vázquez, D. P. & Simberloff, D. Ecological specialization and susceptibility to disturbance: conjectures and refutations. *Am Nat* **159**, 606-623 (2002).
22. Inouye, D. W. & Pyke, G. H. Pollination biology in the Snowy Mountains of Australia: comparisons with montane Colorado, USA. *Austral Ecol* **13**, 191-205 (1988).
23. Bezerra, E. L., Machado, I. C. & Mello, M. A. Pollination networks of oil-flowers: a tiny world within the smallest of all worlds. *J Anim Ecol* **78**, 1096-1101 (2009).
24. de Mendonça Santos, G. M., Aguiar, C. M. L. & Mello, M. A. Flower-visiting guild associated with the Caatinga flora: trophic interaction networks formed by social bees and social wasps with plants. *Apidologie* **41**, 466-475 (2010).
25. Barrett, S. C. & Helenurm, K. The reproductive biology of boreal forest herbs. I. Breeding systems and pollination. *Can J Bot* **65**, 2036-2046 (1987).
26. Hocking, B. Insect-flower associations in the high Arctic with special reference to nectar. *Oikos*, 359-387 (1968).
27. Mosquin, T. & Martin, J. Observations on the pollination biology of plants on Melville Island, NWT, Canada. *Canadian Field Naturalist* **81**, 201-205 (1967).
28. Small, E. Insect pollinators of the Mer Bleue peat bog of Ottawa. *Canadian field-naturalist* (1976).
29. Arroyo, M. T. K., Primack, R. & Armesto, J. Community studies in pollination ecology in the high temperate Andes of central Chile. I. Pollination mechanisms and altitudinal variation. *Am J Bot*, 82-97 (1982).
30. Kaiser-Bunbury, C. N., Memmott, J. & Müller, C. B. Community structure of pollination webs of Mauritian heathland habitats. *Perspect. Plant Ecol. Evol. Syst.* **11**, 241-254 (2009).
31. Olesen, J. M., Eskildsen, L. I. & Venkatasamy, S. Invasion of pollination networks on oceanic islands: importance of invader complexes and endemic super generalists. *Divers Distrib* **8**, 181-192 (2002).
32. Primack, R. B. Insect pollination in the New Zealand mountain flora. *N.Z. J. Bot.* **21**, 317-333 (1983).
33. Dupont, Y. L., Hansen, D. M. & Olesen, J. M. Structure of a plant–flower-visitor network in the high-altitude sub-alpine desert of Tenerife, Canary Islands. *Ecography* **26**, 301-310 (2003).
34. Ollerton, J., Johnson, S. D., Cranmer, L. & Kellie, S. The pollination ecology of an assemblage of grassland asclepiads in South Africa. *Ann Bot* **92**, 807-834 (2003).

35. Elberling, H. & Olesen, J. M. The structure of a high latitude plant- flower visitor system: the dominance of flies. *Ecography* **22**, 314-323 (1999).

36. Dicks, L., Corbet, S. & Pywell, R. Compartmentalization in plant–insect flower visitor webs. *J Anim Ecol* **71**, 32-43 (2002).

37. Schemske, D. W. *et al.* Flowering ecology of some spring woodland herbs. *Ecology* **59**, 351-366 (1978).

38. Ramirez, N. & Brito, Y. Pollination biology in a palm swamp community in the Venezuelan Central Plains. *Bot J Linn Soc* **110**, 277-302 (1992).

Supplementary Table 2. Summary of the GLM addressing the effects of the type of mutualism and the level of mutualistic selection on the contribution of indirect effects to trait evolution. Additional details of this analysis are available in the Supplementary Methods.

	F	df	*P*
Model	837.12	6	< 0.0001
Type of mutualism	194.94	5	< 0.0001
Mutualistic selection	4047.97	1	< 0.0001
Error		593	

Supplementary Table 3. Summary of the GLM addressing the effects of the type of mutualism, the species richness, and the level of mutualistic selection on the contribution of indirect effects to trait evolution. Additional details of this analysis are available in the Supplementary Methods.

	F	df	*P*
Model	846.94	7	< 0.0001
Type of mutualism	117.42	5	< 0.0001
Species richness	96.56	1	< 0.0001
Mutualistic selection	4700.26	1	< 0.0001
Error		592	

Supplementary Table 4. Summary of simple linear regressions addressing the relationships between the indirect effects and two aspects of coevolutionary dynamics as response variables: time-to-equilibrium and the amount of directional change per species per time step. All of the variables were estimated as the residuals of regressions using species richness as an explanatory variable to control for the effects of species richness (n = 75 networks for all analysis). See the Supplementary Methods for further information.

	Time-to-equilibrium	Amount of directional change
slope	301.25	-1.6×10^{-3}
F	40.08	35.06
R^2	0.354	0.324
P	< 0.0001	< 0.0001

Supplementary Table 5. Summary of simple linear regressions addressing the effect of each network metric on the mean contribution of indirect effects to trait evolution (n = 75 networks for all analyses). Species richness was log-transformed prior the analysis. Additional details can be found in the Supplementary Methods (section 3).

	slope	*F*	R^2	*P*
Species Richness	0.081	131.24	0.642	< 0.0001
Connectance	-0.147	3.75	0.049	0.0567
Relative Nestedness	0.114	127.04	0.635	< 0.0001
Relative Modularity	-0.537	91.11	0.555	< 0.0001